

Adaptive Computation Modules: Granular Conditional Computation For Efficient Inference

Bartosz Wójcik
Jagiellonian University
IDEAS NCBR

b.wojcik@doctoral.uj.edu.pl

Pasquale Minervini
University of Edinburgh
University College London

Alessio Devoto
Sapienza University of Rome

Karol Pustelnik
University of Warsaw

Simone Scardapane
Sapienza University of Rome

Abstract

The computational cost of transformer models makes them inefficient in low-latency or low-power applications. While techniques such as quantization or linear attention can reduce the computational load, they may incur a reduction in accuracy. In addition, globally reducing the cost for all inputs may be sub-optimal. We observe that for each layer, the full width of the layer may be needed only for a small subset of tokens inside a batch and that the “effective” width needed to process a token can vary from layer to layer. Motivated by this observation, we introduce the Adaptive Computation Module (ACM), a generic module that dynamically adapts its computational load to match the estimated difficulty of the input on a per-token basis. An ACM consists of a sequence of learners that progressively refine the output of their preceding counterparts. An additional gating mechanism determines the optimal number of learners to execute for each token. We also describe a distillation technique to replace any pre-trained model with an “ACMized” variant. The distillation phase is designed to be highly parallelizable across layers while being simple to plug-and-play into existing networks. Our evaluation of transformer models in computer vision and speech recognition demonstrates that substituting layers with ACMs significantly reduces inference costs without degrading the downstream accuracy for a wide interval of user-defined budgets.

1. Introduction

Driven by their constantly improving capabilities, state-of-the-art neural networks have been experiencing a continued growth in size in the last decade [26]. This progress was made possible both by algorithmic and model design

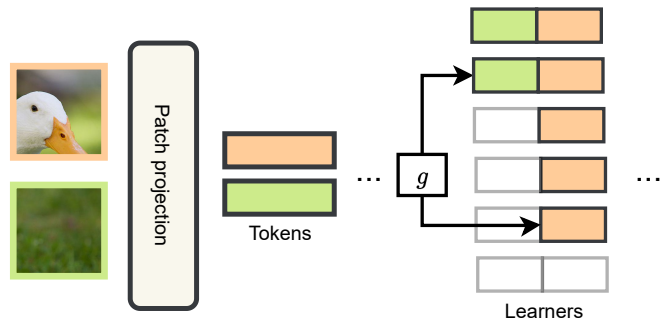


Figure 1. High-level overview of our proposed module: an ACM adapts its computational load for each input on a per-token basis by selecting the number of *learners* to execute through a trainable gate. In the example, a background token (green) is allocated fewer learners than a content-rich token (orange).

improvements (in particular with the introduction of transformer models) and the increasing computational power of modern GPUs. Scaling up the model architecture frequently results in improved performance [11, 44], causing the size and computational costs of state-of-the-art models to keep increasing steadily. These escalating costs not only limit applications in latency-sensitive and energy-constrained scenarios, but also contribute to higher carbon emissions, exacerbating environmental concerns. [25, 33].

Several approaches from the literature aim at mitigating this problem. For example, quantization reduces inference time by quantizing the weights and activations into low-precision floating-point [9] or integer values [10, 40]. Knowledge distillation methods [1, 18] can transfer knowledge from an ensemble or single larger model into a smaller network. Finally, sparsification methods [15, 19, 21] yield either sparse weight, or sparse activation tensors.

While they incur a slight decrease in downstream model performance, such methods show that some neural modules can often be replaced with computationally cheaper alternatives. Based on this observation, we argue that in transformer models [38], the representational capacity of a whole layer is not needed for every input token. In other words, we hypothesize that the same transformation could be achieved in a more computationally efficient manner. To explore this hypothesis, we introduce *Adaptive Computation Modules* (ACMs), a neural network module that adapts its computational burden to match the difficulty of the current input token. An ACM consists of a sequence of *learners* and a single gating network. The task of each learner is to improve upon the combined output of previous learners, while the gating network determines the optimal number of learners to execute for each input token. Since all token-level decisions are independent, the resulting model is a highly granular application of the conditional computation paradigm [5, 6], and thus allows for spatial adaptability in transformer models [14, 16]. Fig. 1 provides an outline of the proposed model. To enable the use of a vast range of publicly available models, we propose a straightforward conversion procedure, in which we: (1) substitute the selected blocks of the model with ACMs, (2) train the learners by distilling knowledge from the substituted blocks, (3) train the gating networks using artificially generated labels, and (4) finetune the entire model in an end-to-end manner.

Our resulting approach can significantly decrease the model’s computational footprint without sacrificing its performance. We evaluate our method on the ImageNet-1k [31] dataset with Vision Transformer (ViT) models and on speech recognition with pre-trained Wav2Vec networks [4], and show that in both cases we achieve a better performance-efficiency trade-off than other conditional computation methods. To summarize, we make the following contributions:

- We introduce ACM, an easy-to-train, modular, and general-purpose module that offers a granular approach for reducing the computational cost of transformers.
- We propose an efficient way for training ACMs that relies on module-wise knowledge distillation from pre-trained models.
- We show that individual layers in transformer models can be computationally inefficient and that their entire expressiveness is often needed only for a small subset of the input tokens.

2. Related Work

We provide a brief overview of related works with a focus on our experimental comparison. A longer overview with a broader outlook can be found in the supplementary material.

Conditional computation Conditional computation (CC)

refers to the ability of a model to adapt its computational graph to its input. While CC can be used for problems such as continual learning [23], most CC methods adjust their execution on a per-input basis to significantly reduce their average computational cost while maintaining performance. In the following, we focus on CC algorithms that can be applied to any pre-trained transformer model with minimal modifications; architecture-specific CC algorithms (e.g., dynamic channel selection for CNNs [8, 22]) are discussed in the supplementary material. We broadly categorize the methods into three groups: early-exits (EEs) [7, 37], mixture-of-experts (MoEs) [13, 34, 42], and token dropping (TD) [17, 24, 29, 41]. We review each of them, highlighting similarities and differences with the proposed ACM model.

Early-exits In EE models, inputs are allowed to “exit” the architecture at intermediate layers via additional classifier heads that are trained together with the backbone network [37], or as a separate phase in a layerwise fashion [16], and the predictions of multiple heads can be merged with a number of different techniques [32, 37, 39]. In EE networks the execution is stopped for the entire input at once, as opposed to individual tokens as is done in the proposed ACMs. In addition, designing and placing exit heads is itself a non-trivial problem [37], and very few work has been done outside standard computer vision and natural language processing classification tasks. In contrast, ACMs are designed to replace individual blocks in a transformer model in a plug-and-play fashion.

Token dropping TD strategies either prematurely stop execution [17, 29, 41] or skip computation of selected layers [24] for *individual tokens* that are deemed less relevant or redundant. We can interpret them as dynamically allocating a variable depth to each token. Our proposed ACM can be seen as an orthogonal *width* variant of token dropping, in which each token is allocated a variable *width* for each layer in the network.

Mixture-of-experts In MoEs, selected modules of a model are replaced by an independent set of blocks called experts, which are selectively activated for each token by an additional routing network [27]. MoEs have been successfully developed for replacing MLP layers in transformer models [30, 34], attention layers [45], entire blocks [36], and adapters [43]. Although MoEs are typically trained from scratch or fine-tuned from existing models [43], a small number of works have investigated *moefication* procedures [28, 46]. Importantly, in MoEs each token is allocated a fixed amount of compute depending on the routing strategy (e.g., top- k routing [30]). ACM can be seen as a modification of MoEs in which the experts are ordered, and thus the complexity of the routing problem being drastically reduced. The gating network decides *how many* learners instead of *which* experts to execute, therefore allowing for a variable amount of computation on a per-token basis.

3. Method

We introduce the ACM architecture in Section 3.1 (see Fig. 2 for reference). An ACM is a conditional computation block that adapts its execution cost for each processed token via a trainable gating layer. In this paper, instead of training an ACM-based model from scratch, we focus on converting *any* pre-trained transformer network into an equivalent “ACMized” version, i.e. one having similar accuracy while achieving a pre-defined computational budget on average. To this end, we propose a customized distillation-based pipeline (Fig. 3). First, we substitute a subset of layers of the base model (e.g., MLPs or MHA projections) with an ACM of similar size. The ACMs are then trained independently but *in parallel*, first with a per-layer reconstruction loss (Section 3.2, Fig. 3a) and then using a cross-entropy loss to initialize the gates (Section 3.3, Fig. 3b). At the last phase we fine-tune the model end-to-end to allow the model to adapt its weight for dynamic inference setting (Section 3.4, Fig. 3c). We have found this setup to work robustly and to significantly speed-up the training of the ACMized networks in all cases.

3.1. Adaptive Computation Module

Our ACM module aims to allow the model to work well with any required computational budget while still ensuring efficient execution on GPUs, a property most of the dynamic width methods lack [22]. Given an input token z , consider a set of N homogeneous modules, $s_n(z; \phi_{(n)})$, $n \in \{1, \dots, N\}$, each module having weights $\phi_{(n)}$. We refer to these modules as *learners*. In an ACM, each learner progressively refines the prediction of the previous ones such that the k -th output of the ACM block, $k \in \{1, \dots, N\}$, is given by:

$$h(z, k; \phi) = \sum_{n=1}^k s_n(z; \phi_{(n)}) \quad (1)$$

All intermediate outputs $h(z, 1; \phi), \dots, h(z, N; \phi)$ are valid choices for the output of the ACM: a larger value for k yields a more accurate result at the cost of a higher computational burden, while $k = 1$ means that only a single learner is executed. Note that once k is known for a token, the learners can be executed in parallel.

For any token z , k should be chosen as the smallest possible value that guarantees a good performance of the network. To this end, at the beginning of the ACM block, we add a small trainable gating network g with weights ω to select the number of learners k to be executed. In practice, the gating network returns N real-valued outputs, which are then discretized into a one-hot gating choice vector with the Gumbel-Softmax trick [20] to retain differentiability:

$$\nu_n = \frac{\exp((\log(g(z; \omega))_n + \gamma_n)/T)}{\sum_n \exp((\log(g(z; \omega))_n + \gamma_n)/T)}. \quad (2)$$

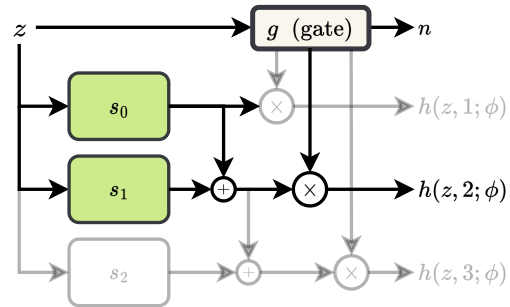


Figure 2. Architecture of an ACM block – the output is given by the sum of k learners, where k is determined on a per-token basis by a small gating network g . The learners can be executed in parallel. In the example, only the first two learners are executed, and the computation of the third (greyed out) is skipped.

In Eq. (2), $\gamma_1, \dots, \gamma_N$ are i.i.d samples from $\text{Gumbel}(0, 1)$, and T is softmax temperature. In the forward pass, we discretize ν into a one-hot vector $\hat{\nu}$, but the continuous values are used directly for gradient computation in the backward pass. The complete ACM architecture is outlined in Fig. 2.

Design of the ACM blocks Any network architecture with the required input and output dimensionality can play the role of a learner. For simplicity, in this paper, we always use two dense layers with a GELU activation function in between. Since we replace selected modules of a pre-trained model with ACMs, we always pick N and the size of a single learner such that the entire ACM module has approximately the same computational cost and the number of parameters as the substituted block. This is straightforward to achieve as the cost of a learner scales linearly with its hidden dimensionality. However, the output dimension has to be the same as in the replaced module. This results with output layer biases taking a larger share of learner parameters as we increase N . To avoid this effect, we simply eliminate them from our architecture.

For the gating network we also use a two-layer network, and determine its hidden dimensionality such that the total computational cost of gating is around 1% of the overall model cost. When feasible – such as the module being placed under a residual connection – we set the minimum number of executable learners to 0 so that even the computation of the first learner can be skipped.

3.2. Module-wise Representation Distillation

The costs of training large models are constantly increasing [35]. On the other hand, there is a large number of publicly available pre-trained models, so the capability of adapting them is a desired property for new methods. Since ACMs are designed to replace individual modules, we initially train them by distilling the knowledge from the correspond-

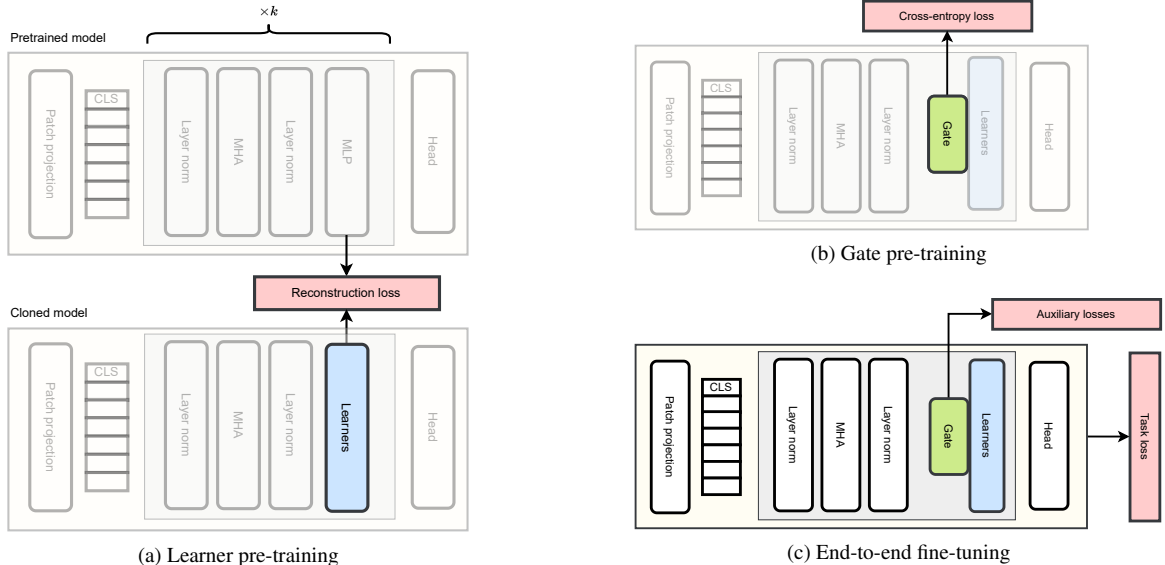


Figure 3. Outline of the proposed pre-trained model conversion pipeline. (a) We clone the pre-trained transformer model and replace the selected modules with ACMs. The learners in each ACM are trained *independently but in parallel* with *module-wise representation distillation*. (b) The gating networks of each ACM are trained in the second stage using artificially generated labels, also in parallel. (c) At the last stage, we train the entire model in an end-to-end manner with auxiliary losses that penalize the deviation from the target average computational budget and enforce diversity of gating choices. The blocks that are not trained in their stage are greyed out. Note that we can optionally also substitute the projection layers in multi-head attention (MHA) blocks with ACMs, which we do not depict here for clarity of presentation. We also omit some architectural details such as residual connections for readability.

ing trained modules that are being substituted. Specifically, we propose the following scheme, outlined in Fig. 3a. A trained static model $f(\cdot)$ is cloned, and selected modules (e.g., every MLP module) are replaced with ACMs in that cloned model $f_{\text{ACMized}}(\cdot)$. Each learner from every ACM is initialized randomly. For each sample x_i from a mini-batch B forwarded through the original model, we save every input token $z_{i,j}^l$ and output token $o_{i,j}^l$ of each l -th module that was replaced in the copied model. Then, every ACM is trained independently and in parallel by minimizing the mean squared error (MSE) applied for every possible choice of k :

$$\mathcal{L}(\phi) = \frac{1}{|B|SLN} \sum_{i,j,l,n} \|h(z_{i,j}^l, n; \phi^l) - o_{i,j}^l\|^2 \quad (3)$$

where S is token sequence length, and L is the number of substituted modules. Note that the gating network is not needed in this phase. The effectiveness of this training approach can be tested by setting a fixed k for every ACM in the model and evaluating the model on the validation set.

3.3. Pre-training the Gating Networks

With learners being able to reliably imitate the replaced modules, we subsequently freeze them and train the gating networks in a similar, layer-wise approach. We frame the problem as a classification task and generate artificial labels

with the following heuristic. First, we consider the outputs of all learners and compute the distance to the original output:

$$d_{i,j}^l(n) = \|h(z_{i,j}^l, n; \phi) - o_{i,j}^l\|_2 \quad (4)$$

The target label is then set as:

$$t_{i,j}^l = \min \left\{ n \in \{2, \dots, N\} \mid \frac{d_{i,j}^l(n)}{d_{i,j}^l(n-1)} \geq \tau \right\}, \quad (5)$$

where τ is a threshold hyperparameter. In other words, we select the smallest number of learners such that the relative improvement from adding one more learner is lower than the threshold τ . With these labels, the gating networks are trained using standard cross-entropy loss:

$$\mathcal{L}(\omega) = \frac{1}{|B|SLN} \sum_{i,j,l,n} -t_{i,j,n}^l \log(v_{i,j,n}^l). \quad (6)$$

We visualized this training step in Fig 3b.

3.4. End-to-end Finetuning

In the third phase, we finetune the entire model end-to-end to allow it to adapt its weights to the dynamic inference setting. To make the model more predictable in terms of its computational cost, we add an auxiliary loss term that penalizes for any deviation from the given target budget β_{target}

on average:

$$\mathcal{L}_b(\theta) = \left\| \frac{1}{|B|} \sum_i \frac{\sum_j \sum_l k_{i,j}^l p^l}{\sum_j \sum_l N p^l} - \beta_{\text{target}} \right\|_1, \quad (7)$$

where p^l is the computational cost of a single learner from layer l and $\beta_{\text{target}} \in (0, 1)$ is the targeted computational budget. This term still allows for the allocation of different amounts of computational resources to samples of varying complexity and only requires to be close to β_{target} *on average*. It also affects the computational cost of future training steps, potentially accelerating the training process.

While \mathcal{L}_b does not prevent diversity of gating choices, it does not encourage it. In practice we find that the gating networks collapse to a state where the same number of learners is chosen for every input token, effectively turning our dynamic model into a static one. To prevent this behavior and encourage diversity, we add two additional loss terms. The first auxiliary loss term maximizes the average normalized entropy of gating choices taken for tokens in a single image:

$$\mathcal{L}_e(\theta) = \frac{1}{|B|L} \sum_{i,l} \frac{\sum_n a_n \log(a_n)}{\log(N)}, \quad (8)$$

where

$$a_{i,n}^l = \frac{\sum_j \hat{v}_{i,j,n}^l}{\sum_n \sum_j \hat{v}_{i,j,n}^l} \quad (9)$$

represents a distribution between N choices in batch B for the l -th ACM aggregated for an entire sequence of tokens from sample i . The intuition behind this loss is that not every input region is equally important; hence, a non-uniform distribution of computation is required.

Finally, entire images may exhibit different difficulty levels, and enforcing diversity of gating choices for a single image at a time may not be enough. We address this with the second auxiliary loss, which is defined as:

$$\mathcal{L}_d(\theta) = \frac{1}{|B|^2} \sum_i \sum_m \|b_i - b_m\|_1, \quad (10)$$

where

$$b_i = \frac{\sum_j \sum_l k_{i,j}^l}{\sum_j \sum_l N} \quad (11)$$

denotes the fraction of learners executed on sample i . It encourages the model to distribute its computational budget between easy and hard examples. The final loss that is minimized for classification tasks is given by:

$$\begin{aligned} \mathcal{L}(\theta) = & \frac{1}{|B|} \sum_i \sum_c -y_{i,c} \log(\hat{y}_{i,c}) + \alpha_b \mathcal{L}_b(\theta) \\ & + \alpha_e \mathcal{L}_e(\theta) + \alpha_d \mathcal{L}_d(\theta), \end{aligned} \quad (12)$$

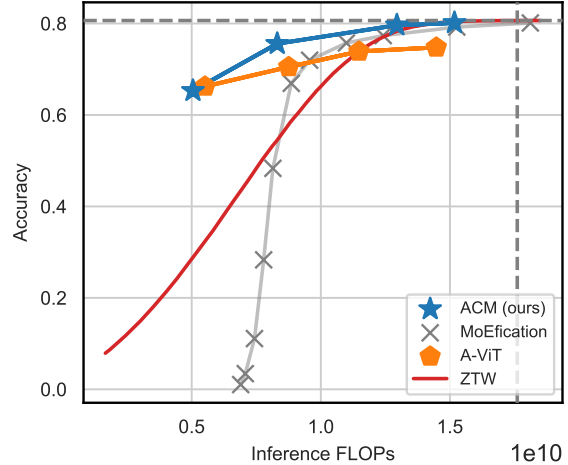


Figure 4. Performance-efficiency trade-offs of different conditional computation methods as measured on the ImageNet-1k dataset. ACM-based ViT-B achieves the Pareto frontier for a wide range of computational budgets.

where $\{(x_i, y_i)\}_{i=1}^{|B|}$ are samples from the current mini-batch B , and $\alpha_b, \alpha_e, \alpha_d$ are hyperparameters for weighting the different terms. In practice, we always use $\alpha_b = 0.1$, $\alpha_e = 0.05$, and $\alpha_d = 0.05$. The finetuning procedure is visualized in Fig. 3c. In Section 5, we present an ablation study that demonstrates the necessity of applying the proposed auxiliary losses and shows the positive impact of their interplay. Note that the auxiliary losses are task-agnostic, allowing ACMs to be used for any other task than classification.

4. Experiments

We evaluate our method on popular image classification and speech recognition tasks due to the widespread availability of pre-trained weights. The aim of the evaluation is to compare the performance-efficiency trade-offs of different methods. For balanced datasets the performance of the models can be directly expressed as accuracy. To measure the computational efficiency, we track the number of FLOPs (floating point operations) used by the model for each sample being evaluated and report the averaged result. Among the compared methods, ACMs are the only models that adjust the computational cost during training. However, as the main aim of ACMs is the reduction of inference costs, in the following, we restrict our evaluation only to inference FLOPs.

The source code for reproducing the experiments presented in this paper is available at https://github.com/bartwojcik/adaptive_computation_modules.

4.1. Computer Vision

We select a ViT-B [12] model pre-trained on ImageNet-1k [31] from the `torchvision` library¹ as the base model for all methods. We compare ACMized models with three conditional computation methods, each one coming from a different group: A-ViT [41] (Token Dropping), MoEfication [46] (Mixture-of-Experts), and Zero Time Waste [39] (Early Exiting). For the sake of a fair comparison, we assume the same training data budget of 100 epochs for every technique.

Since MoEfication requires models using ReLU activation functions, we first replace GELU activations with ReLUs and finetune the model for 80 epochs, as described by Zhang et al. [46]. The remaining 20 epochs are used for training the routers. For Zero Time Waste, we train the early-exit heads for 95 epochs and then train the ensembles for 5 epochs. For the ACMized ViT, we replace every MLP module and every linear projection in each MHA with an ACM module. Module-wise representation distillation is performed for 2 epochs, followed by 1 epoch for pre-training of the gating networks and 97 epochs of end-to-end finetuning of the entire model. We set the number of learners N to 4 in every ACM. While MoEfication and Zero Time Waste can be evaluated with different numbers of selected experts and early exit confidence thresholds, A-ViT and ACMs need to be trained multiple times with different values of hyperparameters that approximately determine the final average computational budget. We emphasize that our A-ViT implementation includes fixes for two issues raised by GitHub users²³, which may affect the final performance of A-ViT. The authors of A-ViT have not yet addressed them at the time of writing of this article.

We present the results in Fig. 4. As projections in MHA are responsible for around 30% of the model cost, MoEfication seems to be hindered by the fact that it reduces only the cost of the MLP layers. A-ViT shows a gap in performance in relation to the pre-trained model, while Zero Time Waste is competitive only for higher computation budgets. On the other hand, ACMized ViT displays favorable performance for a wide range of computational budgets, and its advantage is especially significant below 12.5 GFLOPs.

4.2. Speech-to-Text

For speech recognition tasks, we leverage the pre-trained models from the Huggingface hub⁴. Specifically, we use XLS-R-300M [3], a pre-trained iteration of Wav2Vec2 [4], fine-tuned on selected languages from the CommonVoice dataset [2].

¹<https://pytorch.org/vision/stable/models.html>

²<https://github.com/NVlabs/A-ViT/issues/4>

³<https://github.com/NVlabs/A-ViT/issues/13>

⁴<https://huggingface.co/models>

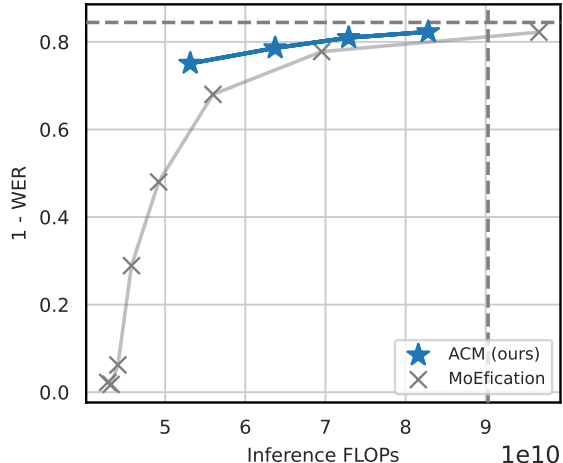


Figure 5. Performance-efficiency trade-offs of different conditional computation methods as measured on the CommonVoice-es dataset. The model’s performance is reported in terms of Word Error Rate (WER). ACMs achieve lower WER for every evaluated computational budget.

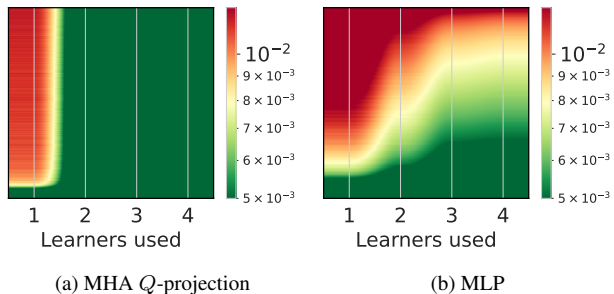


Figure 6. Color-coded errors of a 4-learner ACM plotted after performing module-wise representation distillation for modules from eight block of a ViT-B pre-trained model. Tokens are sorted along the Y axis of the plot by their average error. For most input tokens, the same transformation can be performed by a considerably smaller module consisting of only two or three learners.

Speech-to-text models introduce additional complexities for dynamic computation methods, as each token is decoded individually. Since A-ViT and Zero Time Waste were not designed for this setting, we restrict our baseline methods to MoEfication, the only task-agnostic method among those three.

As in Section 4.1, we assume an equal training data budget of 10 epochs for all approaches. In the case of MoEfication, we substitute GELUs with ReLUs and train for 8 epochs, followed by 2 epochs of router training. For ACMs, we replace every MLP block within the model with an ACM module with $N = 4$. We subsequently perform 5 epochs of module-wise distillation, one 1 of training the gating net-

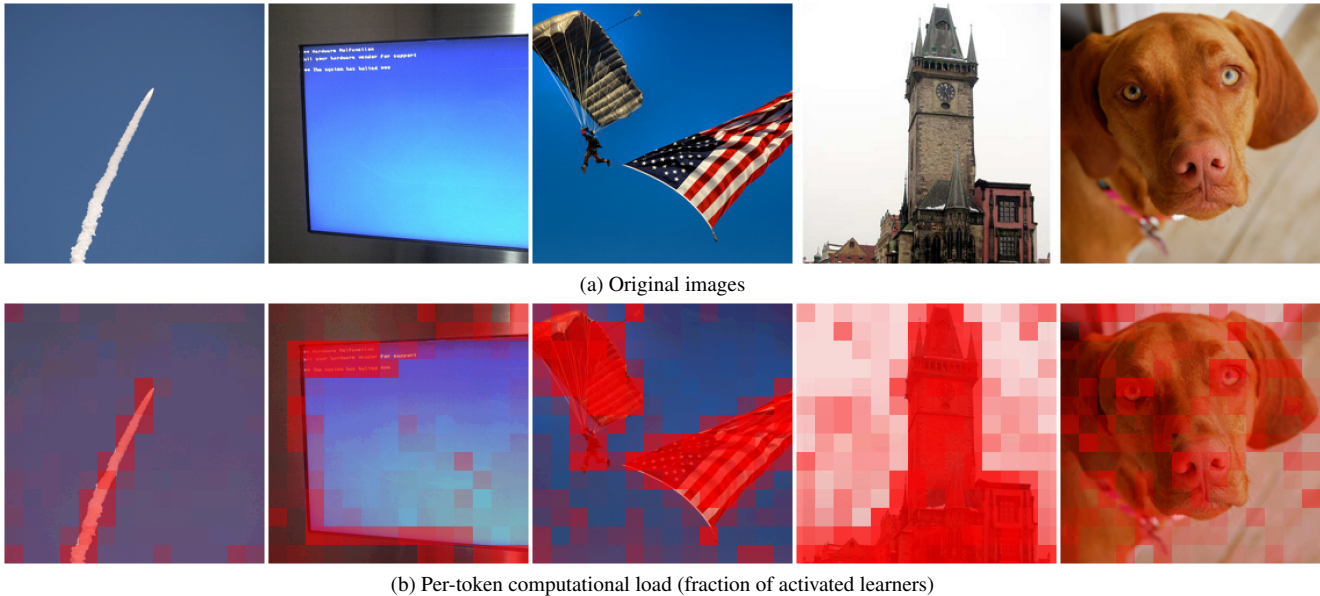


Figure 7. Computational load heatmaps rendered over example images for the model trained with $\beta_{\text{target}} = 0.6$. The model allocates its computational budget to semantically meaningful patches.

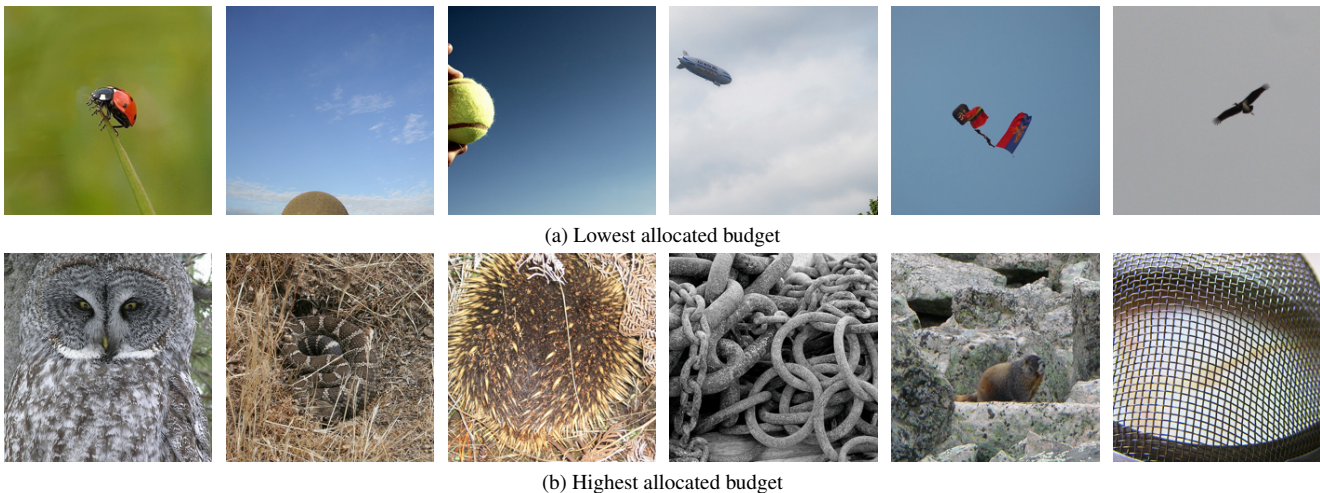


Figure 8. Samples that consumed the least (top row) and most (bottom row) computation of the model trained with $\beta_{\text{target}} = 0.6$. We can see that the model perceives images containing high-frequency content as significantly harder.

works, and 4 epochs of end-to-end finetuning. We present results in Fig. 5. We see that even if only the MLP blocks are ACMized, our method still obtains better performance-efficiency trade-off than MoEfication.

5. Analysis

Compared to static models, dynamic models allocate variable amounts of compute for different samples or input regions. In this section, we examine the distribution of computational load and show that the introduced auxiliary losses are needed. Furthermore, we show that static,

large modules such as MLPs in transformer architectures are computationally inefficient for a majority of their input tokens.

Computational Inefficiency in Static Modules To justify the particular form of the ACM architecture, we make the following experiment. First, we perform module-wise distillation from a selected static module of an ImageNet-1k pre-trained ViT-B into 4 learners, just as we describe in Section 3.2. After convergence, we randomly select 5000 sample images from the validation dataset and forward them through the original model to save every input token $z_{i,j}$

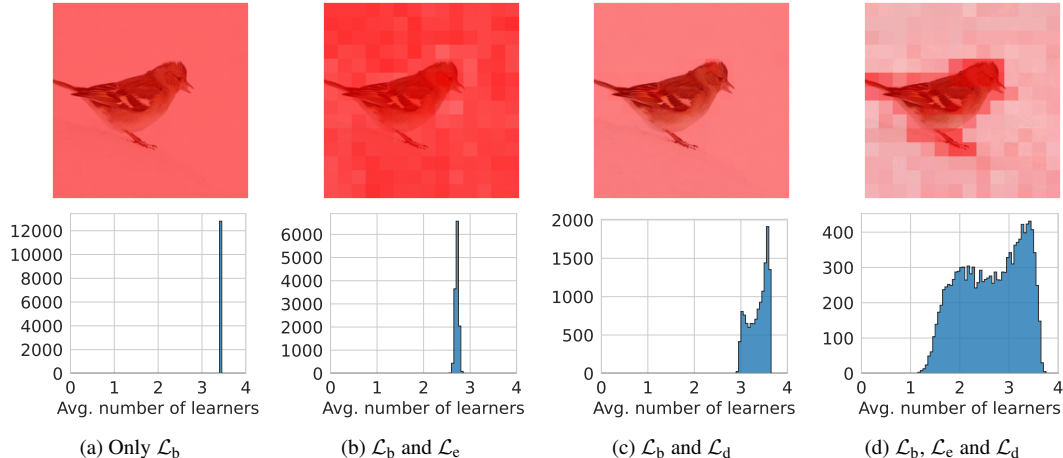


Figure 9. Effects of training with different combinations of enabled auxiliary losses. The histograms (bottom row) show the distribution of the total computational cost spent by the model on images from the validation set. Only combining all the proposed terms provides the desired diversity of the allocated computational budget.

and output token $o_{i,j}$. For every possible number of learners used $n \in \{1, \dots, N\}$, we are interested in how well the learners imitate the output of the original module. For this, as in training, we use MSE: $\|h(z_{i,j}^l, n; \phi^l) - o_i^l\|^2$. The resulting tensor of MSE values has size $(5000, 197, 4)$, where 197 is the sequence length specific to ViT-B with patch size set to 16. Since ACMs process each token independently, we flatten the first two dimensions and then sort the tokens by the average error for readability. Fig. 6 shows the resulting color-coded error visualizations for selected modules. We emphasize that the four learners have approximately the same cost and number of parameters as the original static module being substituted.

The results show that: 1) only a small subset of tokens require the full processing power of the entire module, and for a majority of tokens, the same transformation can be performed by a significantly smaller and computationally cheaper network; 2) tokens usually exhibit varying levels of difficulty, thus warranting the use of conditional computation on a per-token basis.

Qualitative Analysis A dynamical model should take advantage of the fact that images exhibit different difficulty levels for classification. By extracting the gating choices being done by every ACM for each patch, we can plot a mask over the image that indicates which regions the model was focused the most on. The heat map should correlate with the meaningful regions of the image. Fig. 7 presents the results of this analysis. The model mostly learned to ignore blurred and low-frequency content. To further confirm this, we procedurally found validation dataset samples that were the most and least computationally demanding for the model. The images we present in Fig. 8 provide further evidence for this hypothesis.

Ablation Study Being able to dynamically allocate computation when solving a task is the core feature of ACMized models. The auxiliary losses introduced in Section 3.4 are necessary for the dynamism to emerge. We empirically demonstrate this in Fig. 9 by training multiple runs differing only in the loss terms applied during the end-to-end finetuning stage. For each run, we visually analyze their intra-sample computational load distribution and generate a histogram of the total computation spent on every sample. As expected, ACMs may converge to a solution in which always the same learners are used when only \mathcal{L}_b is applied. The inclusion of \mathcal{L}_e helps in diversifying between different regions of the input, but overall the computation spent on each image is mostly the same. Applying \mathcal{L}_d instead of \mathcal{L}_e diversifies the distribution of compute spent on every image, but the gating choices for different regions of the input are not diverse on its own. Only by enabling all the proposed losses can we achieve the desired effect of the model focusing on semantically meaningful patches and having a high variability of computational budget allocation.

6. Limitations

While the proposed distillation-based pre-training procedure converges relatively quickly, it requires keeping both models in memory simultaneously, potentially limiting its application. Furthermore, similarly to Mixture-of-Experts, ACMs require a tuned custom implementation to utilize GPUs efficiently.

7. Conclusion

In this work, we have demonstrated that large static modules lead to ineffective allocation of computational budget. The introduced ACM, a generic module that facilitates granular

conditional computation, is designed for computational effectiveness, and models based on it achieve state-of-the-art results among the tested dynamic inference methods. Our training procedure distills a static network into an adaptive one, forcing it to allocate its computational budget to semantically meaningful input regions. In our future work, we plan to explore the relationship between ACMs and pruning methods. Since our training procedure replaces individual modules with ACMs, one could also consider using quantized learners for even further efficiency gains. Finally, ACMs could be potentially helpful in accelerating from-scratch training.

References

- [1] Gustavo Aguilar, Yuan Ling, Yu Zhang, Benjamin Yao, Xing Fan, and Chenlei Guo. Knowledge distillation from internal representations. In *Proceedings of the AAAI Conference on Artificial Intelligence*, pages 7350–7357, 2020. [1](#)
- [2] Rosana Ardila, Megan Branson, Kelly Davis, Michael Henretty, Michael Kohler, Josh Meyer, Reuben Morais, Lindsay Saunders, Francis M. Tyers, and Gregor Weber. Common voice: A massively-multilingual speech corpus. *arXiv preprint at arXiv::1912.06670*, 2020. [6](#)
- [3] Arun Babu, Changhan Wang, Andros Tjandra, Kushal Lakhotia, Qiantong Xu, Naman Goyal, Kritika Singh, Patrick von Platen, Yatharth Saraf, Juan Pino, Alexei Baevski, Alexis Conneau, and Michael Auli. Xls-r: Self-supervised cross-lingual speech representation learning at scale. *arXiv preprint at arXiv::2111.09296*, 2021. [6](#)
- [4] Alexei Baevski, Henry Zhou, Abdelrahman Mohamed, and Michael Auli. wav2vec 2.0: A framework for self-supervised learning of speech representations. *arXiv preprint at arXiv::2006.11477*, 2020. [2](#), [6](#)
- [5] Emmanuel Bengio, Pierre-Luc Bacon, Joelle Pineau, and Doina Precup. Conditional computation in neural networks for faster models. *arXiv preprint arXiv:1511.06297*, 2015. [2](#)
- [6] Yoshua Bengio. Deep learning of representations: Looking forward. In *International conference on statistical language and speech processing*, pages 1–37. Springer, 2013. [2](#)
- [7] Tolga Bolukbasi, Joseph Wang, Ofer Dekel, and Venkatesh Saligrama. Adaptive neural networks for efficient inference. In *International Conference on Machine Learning*, pages 527–536. PMLR, 2017. [2](#)
- [8] Zhoung Chen, Yang Li, Samy Bengio, and Si Si. You look twice: Gaternet for dynamic filter selection in cnns. In *Proceedings of the IEEE/CVF Conference on Computer Vision and Pattern Recognition*, pages 9172–9180, 2019. [2](#)
- [9] Matthieu Courbariaux, Yoshua Bengio, and Jean-Pierre David. Training deep neural networks with low precision multiplications. *arXiv preprint arXiv:1412.7024*, 2014. [1](#)
- [10] Tim Dettmers, Mike Lewis, Younes Belkada, and Luke Zettlemoyer. Llm.int8(): 8-bit matrix multiplication for transformers at scale. *arXiv preprint arXiv:2208.07339*, 2022. [1](#)
- [11] Jacob Devlin, Ming-Wei Chang, Kenton Lee, and Kristina Toutanova. Bert: Pre-training of deep bidirectional transformers for language understanding. *arXiv preprint arXiv:1810.04805*, 2018. [1](#)
- [12] Alexey Dosovitskiy, Lucas Beyer, Alexander Kolesnikov, Dirk Weissenborn, Xiaohua Zhai, Thomas Unterthiner, Mostafa Dehghani, Matthias Minderer, Georg Heigold, Sylvain Gelly, et al. An image is worth 16x16 words: Transformers for image recognition at scale. In *International Conference on Learning Representations*, 2020. [6](#)
- [13] William Fedus, Jeff Dean, and Barret Zoph. A review of sparse expert models in deep learning. *arXiv preprint arXiv:2209.01667*, 2022. [2](#)
- [14] Michael Figurnov, Maxwell D Collins, Yukun Zhu, Li Zhang, Jonathan Huang, Dmitry Vetrov, and Ruslan Salakhutdinov. Spatially adaptive computation time for residual networks. In *Proceedings of the IEEE conference on computer vision and pattern recognition*, pages 1039–1048, 2017. [2](#)
- [15] Song Han, Jeff Pool, John Tran, and William Dally. Learning both weights and connections for efficient neural network. *Advances in neural information processing systems*, 28, 2015. [1](#)
- [16] Yizeng Han, Gao Huang, Shiji Song, Le Yang, Honghui Wang, and Yulin Wang. Dynamic neural networks: A survey. *IEEE Transactions on Pattern Analysis and Machine Intelligence*, 44(11):7436–7456, 2021. [2](#)
- [17] Joakim Bruslund Haurum, Sergio Escalera, Graham W Taylor, and Thomas B Moeslund. Which tokens to use? investigating token reduction in vision transformers. *arXiv preprint arXiv:2308.04657*, 2023. [2](#)
- [18] Geoffrey Hinton, Oriol Vinyals, and Jeff Dean. Distilling the knowledge in a neural network. *arXiv preprint arXiv:1503.02531*, 2015. [1](#)
- [19] Torsten Hoefler, Dan Alistarh, Tal Ben-Nun, Nikoli Dryden, and Alexandra Peste. Sparsity in deep learning: Pruning and growth for efficient inference and training in neural networks. *The Journal of Machine Learning Research*, 22(1):10882–11005, 2021. [1](#)
- [20] Eric Jang, Shixiang Gu, and Ben Poole. Categorical reparameterization with gumbel-softmax. *arXiv preprint arXiv:1611.01144*, 2016. [3](#)
- [21] Yann LeCun, John Denker, and Sara Solla. Optimal brain damage. *Advances in neural information processing systems*, 2, 1989. [1](#)
- [22] Changlin Li, Guangrun Wang, Bing Wang, Xiaodan Liang, Zhihui Li, and Xiaojun Chang. Dynamic slimmable network. In *Proceedings of the IEEE/CVF Conference on computer vision and pattern recognition*, pages 8607–8617, 2021. [2](#), [3](#)
- [23] Min Lin, Jie Fu, and Yoshua Bengio. Conditional computation for continual learning. *arXiv preprint arXiv:1906.06635*, 2019. [2](#)
- [24] Lingchen Meng, Hengduo Li, Bor-Chun Chen, Shiyi Lan, Zuxuan Wu, Yu-Gang Jiang, and Ser-Nam Lim. Adavit: Adaptive vision transformers for efficient image recognition. In *Proceedings of the IEEE/CVF Conference on Computer Vision and Pattern Recognition*, pages 12309–12318, 2022. [2](#)
- [25] David Patterson, Joseph Gonzalez, Urs Hölzle, Quoc Le, Chen Liang, Lluis-Miquel Munguia, Daniel Rothchild,

- David So, Maud Texier, and Jeff Dean. The carbon footprint of machine learning training will plateau, then shrink. *arXiv preprint arXiv:2204.05149*, 2022. 1
- [26] Raffaele Pugliese, Stefano Regondi, and Riccardo Marini. Machine learning-based approach: Global trends, research directions, and regulatory standpoints. *Data Science and Management*, 2021. 1
- [27] Joan Puigcerver, Carlos Riquelme, Basil Mustafa, and Neil Houlsby. From sparse to soft mixtures of experts. *arXiv preprint arXiv:2308.00951*, 2023. 2
- [28] Zihan Qiu, Zeyu Huang, and Jie Fu. Emergent mixture-of-experts: Can dense pre-trained transformers benefit from emergent modular structures? *arXiv preprint arXiv:2310.10908*, 2023. 2
- [29] Yongming Rao, Wenliang Zhao, Benlin Liu, Jiwen Lu, Jie Zhou, and Cho-Jui Hsieh. Dynamicvit: Efficient vision transformers with dynamic token sparsification. *Advances in neural information processing systems*, 34:13937–13949, 2021. 2
- [30] Carlos Riquelme, Joan Puigcerver, Basil Mustafa, Maxim Neumann, Rodolphe Jenatton, André Susano Pinto, Daniel Keysers, and Neil Houlsby. Scaling vision with sparse mixture of experts. *Advances in Neural Information Processing Systems*, 34:8583–8595, 2021. 2
- [31] Olga Russakovsky, Jia Deng, Hao Su, Jonathan Krause, Sanjeev Satheesh, Sean Ma, Zhiheng Huang, Andrej Karpathy, Aditya Khosla, Michael Bernstein, Alexander C. Berg, and Li Fei-Fei. ImageNet Large Scale Visual Recognition Challenge. *International Journal of Computer Vision (IJCV)*, 115(3):211–252, 2015. 2, 6
- [32] Simone Scardapane, Danilo Comminiello, Michele Scarpiniti, Enzo Baccarelli, and Aurelio Uncini. Differentiable branching in deep networks for fast inference. In *ICASSP 2020-2020 IEEE International Conference on Acoustics, Speech and Signal Processing (ICASSP)*, pages 4167–4171. IEEE, 2020. 2
- [33] Roy Schwartz, Jesse Dodge, Noah A. Smith, and Oren Etzioni. Green AI. *Commun. ACM*, 63(12):54–63, 2020. 1
- [34] Noam Shazeer, Azalia Mirhoseini, Krzysztof Maziarz, Andy Davis, Quoc Le, Geoffrey Hinton, and Jeff Dean. Outrageously large neural networks: The sparsely-gated mixture-of-experts layer. *arXiv preprint arXiv:1701.06538*, 2017. 2
- [35] Emma Strubell, Ananya Ganesh, and Andrew McCallum. Energy and policy considerations for deep learning in nlp. *arXiv preprint arXiv:1906.02243*, 2019. 3
- [36] Shawn Tan, Yikang Shen, Zhenfang Chen, Aaron Courville, and Chuang Gan. Sparse universal transformer. *arXiv preprint arXiv:2310.07096*, 2023. 2
- [37] Surat Teerapittayanon, Bradley McDanel, and Hsiang-Tsung Kung. Branchynet: Fast inference via early exiting from deep neural networks. In *2016 23rd international conference on pattern recognition (ICPR)*, pages 2464–2469. IEEE, 2016. 2
- [38] Ashish Vaswani, Noam Shazeer, Niki Parmar, Jakob Uszkoreit, Llion Jones, Aidan N Gomez, Łukasz Kaiser, and Illia Polosukhin. Attention is all you need. *Advances in neural information processing systems*, 30, 2017. 2
- [39] Maciej Wołczyk, Bartosz Wójcik, Klaudia Bałazy, Igor T Podolak, Jacek Tabor, Marek Śmieja, and Tomasz Trzcinski. Zero time waste: Recycling predictions in early exit neural networks. *Advances in Neural Information Processing Systems*, 34:2516–2528, 2021. 2, 6
- [40] Hao Wu, Patrick Judd, Xiaojie Zhang, Mikhail Isaev, and Paulius Micikevicius. Integer quantization for deep learning inference: Principles and empirical evaluation. *arXiv preprint arXiv:2004.09602*, 2020. 1
- [41] Hongxu Yin, Arash Vahdat, Jose M Alvarez, Arun Mallya, Jan Kautz, and Pavlo Molchanov. A-vit: Adaptive tokens for efficient vision transformer. In *Proceedings of the IEEE/CVF Conference on Computer Vision and Pattern Recognition*, pages 10809–10818, 2022. 2, 6
- [42] Seniha Esen Yuksel, Joseph N Wilson, and Paul D Gader. Twenty years of mixture of experts. *IEEE transactions on neural networks and learning systems*, 23(8):1177–1193, 2012. 2
- [43] Ted Zadouri, Ahmet Üstün, Arash Ahmadian, Beyza Ermiş, Acyr Locatelli, and Sara Hooker. Pushing mixture of experts to the limit: Extremely parameter efficient moe for instruction tuning. *arXiv preprint arXiv:2309.05444*, 2023. 2
- [44] Sergey Zagoruyko and Nikos Komodakis. Wide residual networks. In *British Machine Vision Conference 2016*. British Machine Vision Association, 2016. 1
- [45] Xiaofeng Zhang, Yikang Shen, Zeyu Huang, Jie Zhou, Wenge Rong, and Zhang Xiong. Mixture of attention heads: Selecting attention heads per token. *arXiv preprint arXiv:2210.05144*, 2022. 2
- [46] Zhengyan Zhang, Yankai Lin, Zhiyuan Liu, Peng Li, Maosong Sun, and Jie Zhou. Moefication: Transformer feed-forward layers are mixtures of experts. *arXiv preprint arXiv:2110.01786*, 2021. 2, 6

1. Related Work (Extended)

Conditional computation Conditional computation [5, 6] (CC) refers to a broad class of algorithms that make neural networks more efficient by conditioning their computational graph on the specific input, under the hypothesis that inputs with different complexity can require different amounts of compute. This is in contrast to methods such as quantization [12, 14, 51], pruning [21], or knowledge distillation [2, 16, 20], in which a network is replaced entirely by another network having a smaller cost, potentially hindering its performance whenever more flexibility is needed. In principle, networks with CC mechanisms can dynamically adapt their execution on a per-input or per-token basis, significantly reducing their average cost while maintaining performance. Notable examples of CC techniques include dynamic channel selection in CNNs [10, 26], spatial masking of convolutions [47], variable-sized kernels [48], conditional execution of layers [4, 17], dynamic input resizing [49, 61], or combinations of them [1, 29, 52]. The majority of these techniques, however, rely on specific architectural choices, requiring a significant redesign of the model or a separate retraining step. In addition, theoretical speedups are challenging to achieve on modern hardware because the resulting sparsity patterns tend to be unstructured [26]. In contrast, our proposed ACM execution is fully parallelized and provides significant gains without requiring complicated GPU kernels.

Early-exit Models Thanks to their simplicity, early-exit (EE) models are a popular class of CC techniques [7, 45]. In an EE model, inputs are allowed to ‘exit’ the architecture at intermediate layers via additional classifiers taking as input the corresponding hidden representations. These auxiliary blocks can be trained together with the backbone network [45], or as a separate step in a layerwise fashion [18]. Predictions at different levels can be differentiated based on their confidence [45], or combined via geometric [50] or trainable [39] ensembling. EE models have been applied in a number of contexts including language modeling [40] and vision-language applications [44]. While pre-trained models can be converted to EE models by separately training the auxiliary branches, designing and placing the exits is itself a non-trivial task [45], and the majority of solutions are specialized to classification problems. By contrast, the proposed ACM model can be applied seamlessly to any pre-trained Transformer architecture.

Token Dropping Standard EE models stop the processing of the entire input (e.g., image) at once. Separately from this, multiple *token dropping* strategies have been devised to prematurely stop execution on tokens that are deemed less relevant or redundant [19, 29, 36, 53]. Roughly, most

token dropping models dynamically allocate variable network depths to each token. Our proposed ACM can be seen as an orthogonal *width* variant of token dropping, in which each token is allocated a variable *width* for each layer in the network. Some authors have also investigated token merging (instead of dropping) to reduce the number of processed tokens at each block [8, 9, 37].

Mixture-of-Experts Another closely connected CC technique is mixture-of-experts (MoEs) [15, 41, 54]. In a MoE, specific parts of a model are replaced by a block-wise architecture and a routing module that selectively activates specific blocks (‘experts’) for each token [34]. MoEs have been successfully developed for replacing MLP layers in transformers [38, 41], attention layers [58], entire blocks [43], and adapters [56]. In the majority of cases routing is done by activating the top- k most similar experts for each token [38], but many other choices have been proposed including linear assignment problems [13], expert choice routing [60], BASE layers [25], and even soft combinations of inputs [34] or experts’ weights [30]. Also, most MoE models are designed to be trained from scratch, although a small amount of work have investigated *moefication* procedures [35, 59], or fine-tuning with MoEs blocks [56]. While MoEs and the proposed ACM bear some similarity, the design principles of ACMs are significantly different, since each learner acts on the output of previous learners. As a result, in MoEs the computational budget for each token is fixed and depends on the routing strategy (e.g., for top- k routing, exactly k experts will activate), while ACMs exploit the learners’ ordering to allocate a variable number of them to each token. Finally, the simple design of ACM does not suffer from representation collapse issues [11], which is a common problem in MoEs. As a side note, in the limit of replacing individual linear layers (e.g., key-value projections in attention) with smaller linear experts, our work connects to the broader topic of matrix decomposition using low-rank terms, which is gaining prominence in parameter-efficient fine-tuning [22, 27]. However, we empirically validate that using small MLPs as learners is beneficial also for replacing linear blocks.

Discrete Latent Learning In general, CC approaches (including EE and MoE layers) are examples of the emerging field called *modular deep learning* [33], aiming at designing neural networks with more flexible, decomposable architectures for improving efficiency, interpretability, and re-use. A fundamental task in modular NNs is how to take discrete decisions (e.g., sampling experts in MoEs) in a differentiable way for end-to-end training [31]. When sampling from a categorical distribution, this can be done easily via the Gumbel-softmax estimator [23] (also known as the concrete distribution [28]), with similar relaxations existing for

	Phase I	Phase II	Phase III
epochs	2	1	97
$ B $	64	64	512
optimizer	Adam	Adam	Adam
η	10^{-3}	10^{-2}	10^{-4}
scheduler	cosine	cosine	cosine
η_{\min}	10^{-6}	10^{-6}	10^{-6}
clip_grad_norm	1.0	1.0	1.0
T	-	0.8	0.8
τ	-	1.2	-
β_{target}	-	-	{0.25, 0.40, 0.60, 0.75}
α_b	-	-	0.1
α_d	-	-	0.05
α_e	-	-	0.05

Table 1. Hyperparameters used in computer vision experiments presented in the main paper.

top- k sampling [3, 24]. However, sampling a generic element from the powerset of a set is a combinatorial problem, requiring specialized solutions [32]. In the proposed ACM, we sidestep this issue by a proper ordering of the learners, so that sampling a subset of them can be cast as a simpler interval selection problem.

2. Training Details

In Tab. 1 we list the hyperparameters that we used for computer vision experiments. We use the augmentation introduced by Touvron et al. [46], along with mixup ($\alpha_{\text{mixup}} = 0.8$) [57], cutmix ($\alpha_{\text{cutmix}} = 0.8$) [55] and label smoothing ($\epsilon = 0.1$) [42]. Each ACM consists of 4 learners and has approximately the same computational cost as the substituted module. We replace every linear projection of each MHA layer, and each FFN module with an ACM. Due to the presence of residual connections, in every ACM that replaced a FFN module we allow the gating network to activate 0 learners. In contrast, ACMs that replaced projections in MHA layers always have to execute at least one learner for each token.

We list the hyperparameters used for speech-to-text experiments in Tab. 2. This time we replace only the FFN modules, but we also allow for 0 learners to be executed on some tokens.

3. Impact of pre-training

One might hypothesize that the module-wise representation distillation (phase I) and gating networks pre-training (phase II) phases are not necessary. To show their usefulness, we compare our ACMized ViT-B training run with $\beta_{\text{target}} = 0.6$ from the main paper with to two alternative

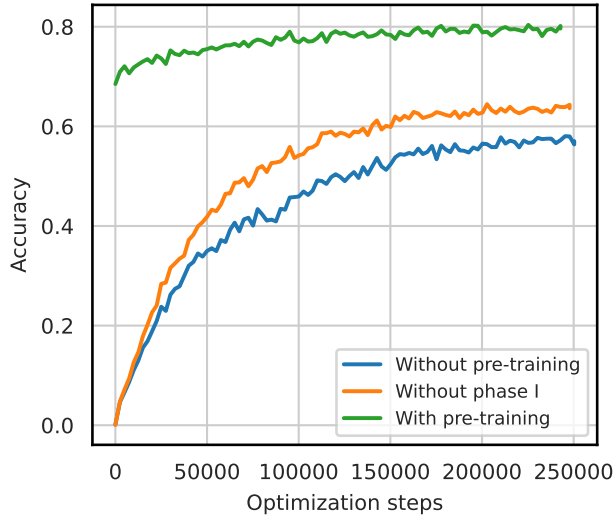
	Phase I	Phase II	Phase III
epochs	5	1	4
$ B $	12	16	16
optimizer	Adam	Adam	Adam
η	$3 * 10^{-4}$	$3 * 10^{-3}$	$3 * 10^{-4}$
scheduler	cosine	cosine	cosine
η_{\min}	10^{-6}	10^{-6}	10^{-6}
clip_grad_norm	1.0	1.0	1.0
T	-	0.8	0.8
τ	-	1.2	-
β_{target}	-	-	{0.25, 0.40, 0.60, 0.75}
α_b	-	-	0.1
α_d	-	-	0.05
α_e	-	-	0.05

Table 2. Hyperparameters used in speech-to-text experiments presented in the main paper.

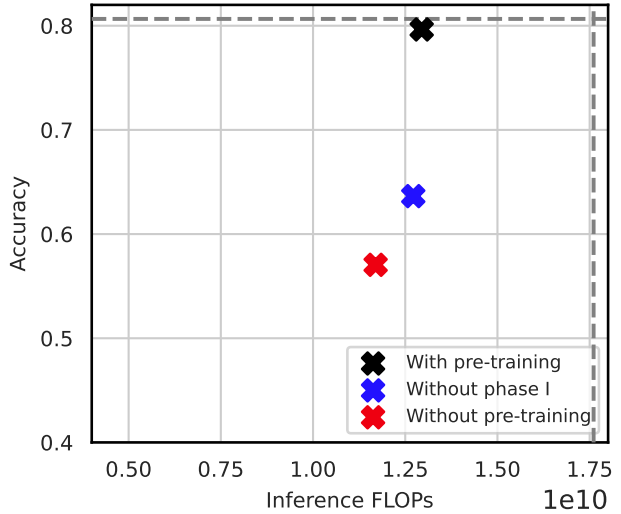
training approaches: (1) end-to-end finetuning only, and (2) without module-wise representation distillation stage. In all cases, the total number of training epochs remains constant (100 epochs), and we always use 2 epochs for module-wise representation-distillation and 1 epoch for gating network pre-training, if they are present. In Fig. 1 we report results of this experiment. Pre-trained gating networks enable faster training in comparison to fine-tuning with randomly initialized parameters. Both stages together provide the intended effect of significantly accelerated training.

4. Choosing N

Due to space constraints, in the main paper we did not explain the reasons for our selection of number of learners N hyperparameter, which we originally set to 4. Here we present a short experiment justifying our selection of this value. We perform the conversion process for different number of learners $N \in \{2, 4, 8, 16\}$ on the same ViT-B model as in our main experiments, with the only difference being that we finetune (third stage) them only for 5 epochs instead of 97 epochs. As before, the total size in parameters and the computational cost of an ACM is always kept approximately close to the original substituted module. Tab. 3 lists the results after the module-wise representation distillation stage, while Fig. 2 presents the final results after finetuning. We highlight two visible effects: (1) fine-grained learners (higher N) have downgraded performance in comparison to coarse-grained learners, and (2) too low N reduces the flexibility of the model in terms of adjustment its computational budget. We pick $N = 4$ as it exhibits the best trade-off that balances these two effects.



(a) End-to-end fine-tuning training curves



(b) Performance-cost result

Figure 1. Analysis of the impact of the proposed three-phase training. Applying both pre-training stages significantly accelerates training in comparison to training the model only with end-to-end fine-tuning.

N	$\frac{k}{N} = 0.25$	$\frac{k}{N} = 0.5$	$\frac{k}{N} = 0.75$	$\frac{k}{N} = 1.0$
2	-	68.37%	-	75.18%
4	41.49%	65.37%	70.65%	71.98%
8	37.62%	62.53%	67.43%	68.84%
16	33.38%	56.61%	62.05%	63.78%

Table 3. ImageNet-1k accuracy scores of ACMized models after first phase of pre-training for different number of learners N that each ACM consists of.

5. Speech-to-text computational load

In the main paper we presented a qualitative analysis for visual data that demonstrated that the model learned to focus its computational resources on semantically important regions of the image (see Fig. 7 in the main paper). In this section we explore whether a similar effect occurs for speech-to-text audio samples. In Fig. 3 we present the average computational load of each token displayed along with the waveform for selected samples from the validation dataset. We can see that in general the model allocates more learners to tokens corresponding to speech, whereas it keeps a low budget for tokens corresponding to silence or background noise.

6. Additional computational load heatmaps

We show in Fig. 4 additional heatmaps for our method, which highlight total amount of activated learners across all layers of the ACMized model for each patch (see Fig. 7 in

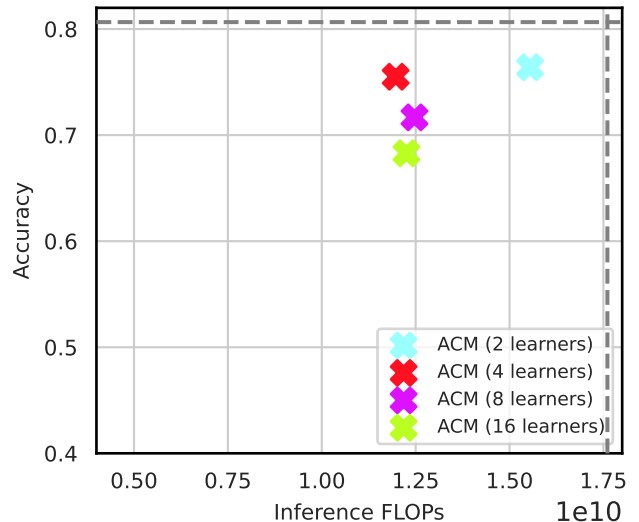


Figure 2. Final performance-efficiency trade-offs of ACMized models with different N after finetuning them for 5 epochs.

the main paper). We can see the model allocates almost zero budget to simple background patches, while for the rest of the images the amount of activated learners correlates with the visual complexity of the objects.

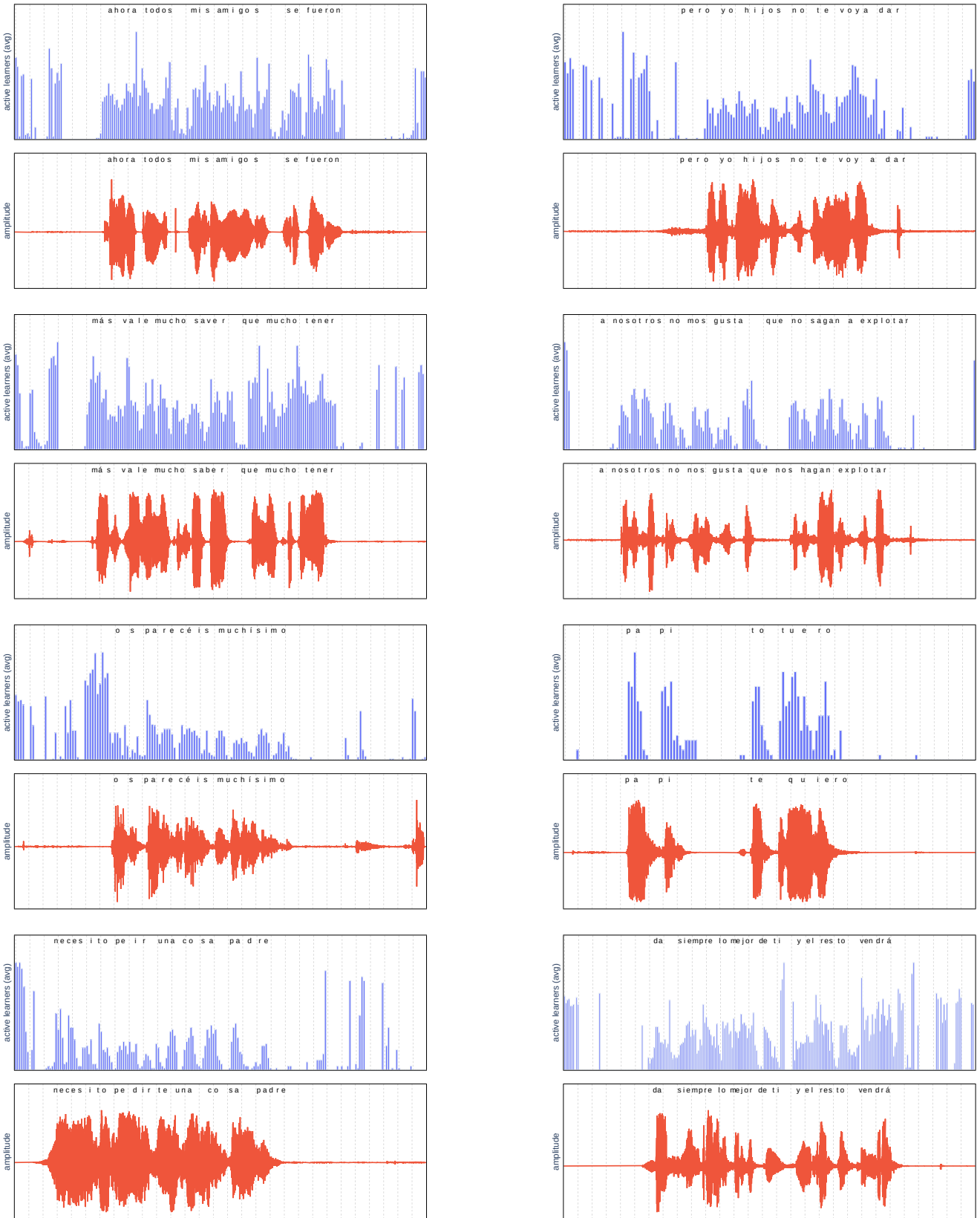


Figure 3. Computational load for each input token for audio models. For each input speech recording (bottom), we show (top) the total number of learners that were activated in the ACMized model.



Figure 4. Computational load heatmaps for additional samples from ImageNet-1k validation dataset. For each image, we show on the right the average fraction of learners that were activated in the ACMized model (the ‘computational load’ of each token).

References

- [1] Samira Abnar, Omid Saremi, Laurent Dinh, Shantel Wilson, Miguel Angel Bautista, Chen Huang, Vimal Thilak, Etai Litwin, Jiatao Gu, Josh Susskind, et al. Adaptivity and modularity for efficient generalization over task complexity. *arXiv preprint arXiv:2310.08866*, 2023. **1**
- [2] Gustavo Aguilar, Yuan Ling, Yu Zhang, Benjamin Yao, Xing Fan, and Chenlei Guo. Knowledge distillation from internal representations. In *Proceedings of the AAAI Conference on Artificial Intelligence*, pages 7350–7357, 2020. **1**
- [3] Kareem Ahmed, Zhe Zeng, Mathias Niepert, and Guy Van den Broeck. SIMPLE: A gradient estimator for k -subset sampling. *arXiv preprint arXiv:2210.01941*, 2022. **2**
- [4] Joshua Ainslie, Tao Lei, Michiel de Jong, Santiago Ontañón, Siddhartha Brahma, Yury Zemlyanskiy, David Uthus, Mandy Guo, James Lee-Thorp, Yi Tay, et al. Colt5: Faster long-range transformers with conditional computation. *arXiv preprint arXiv:2303.09752*, 2023. **1**
- [5] Emmanuel Bengio, Pierre-Luc Bacon, Joelle Pineau, and Doina Precup. Conditional computation in neural networks for faster models. *arXiv preprint arXiv:1511.06297*, 2015. **1**
- [6] Yoshua Bengio, Nicholas Léonard, and Aaron Courville. Estimating or propagating gradients through stochastic neurons for conditional computation. *arXiv preprint arXiv:1308.3432*, 2013. **1**
- [7] Tolga Bolukbasi, Joseph Wang, Ofer Dekel, and Venkatesh Saligrama. Adaptive neural networks for efficient inference. In *International Conference on Machine Learning*, pages 527–536. PMLR, 2017. **1**
- [8] Daniel Bolya and Judy Hoffman. Token merging for fast stable diffusion. In *Proceedings of the IEEE/CVF Conference on Computer Vision and Pattern Recognition*, pages 4598–4602, 2023. **1**
- [9] Daniel Bolya, Cheng-Yang Fu, Xiaoliang Dai, Peizhao Zhang, Christoph Feichtenhofer, and Judy Hoffman. Token merging: Your vit but faster. *arXiv preprint arXiv:2210.09461*, 2022. **1**
- [10] Zhouong Chen, Yang Li, Samy Bengio, and Si Si. You look twice: Gaternet for dynamic filter selection in cnns. In *Proceedings of the IEEE/CVF Conference on Computer Vision and Pattern Recognition*, pages 9172–9180, 2019. **1**
- [11] Zewen Chi, Li Dong, Shaohan Huang, Damai Dai, Shuming Ma, Barun Patra, Saksham Singhal, Payal Bajaj, Xia Song, Xian-Ling Mao, et al. On the representation collapse of sparse mixture of experts. *Advances in Neural Information Processing Systems*, 35:34600–34613, 2022. **1**
- [12] Matthieu Courbariaux, Yoshua Bengio, and Jean-Pierre David. Training deep neural networks with low precision multiplications. *arXiv preprint arXiv:1412.7024*, 2014. **1**
- [13] Damai Dai, Li Dong, Shuming Ma, Bo Zheng, Zhifang Sui, Baobao Chang, and Furu Wei. StableMoE: Stable routing strategy for mixture of experts. *arXiv preprint arXiv:2204.08396*, 2022. **1**
- [14] Tim Dettmers and Luke Zettlemoyer. The case for 4-bit precision: k-bit inference scaling laws. In *International Conference on Machine Learning*, pages 7750–7774. PMLR, 2023. **1**
- [15] William Fedus, Jeff Dean, and Barret Zoph. A review of sparse expert models in deep learning. *arXiv preprint arXiv:2209.01667*, 2022. **1**
- [16] Jianping Gou, Baosheng Yu, Stephen J Maybank, and Dacheng Tao. Knowledge distillation: A survey. *International Journal of Computer Vision*, 129:1789–1819, 2021. **1**
- [17] Alex Graves. Adaptive computation time for recurrent neural networks. *arXiv preprint arXiv:1603.08983*, 2016. **1**
- [18] Yizeng Han, Gao Huang, Shiji Song, Le Yang, Honghui Wang, and Yulin Wang. Dynamic neural networks: A survey. *IEEE Transactions on Pattern Analysis and Machine Intelligence*, 44(11):7436–7456, 2021. **1**
- [19] Joakim Bruslund Haurum, Sergio Escalera, Graham W Taylor, and Thomas B Moeslund. Which tokens to use? investigating token reduction in vision transformers. *arXiv preprint arXiv:2308.04657*, 2023. **1**
- [20] Geoffrey Hinton, Oriol Vinyals, and Jeff Dean. Distilling the knowledge in a neural network. *arXiv preprint arXiv:1503.02531*, 2015. **1**
- [21] Torsten Hoefler, Dan Alistarh, Tal Ben-Nun, Nikoli Dryden, and Alexandra Peste. Sparsity in deep learning: Pruning and growth for efficient inference and training in neural networks. *The Journal of Machine Learning Research*, 22(1): 10882–11005, 2021. **1**
- [22] Edward J Hu, Yelong Shen, Phillip Wallis, Zeyuan Allen-Zhu, Yuanzhi Li, Shean Wang, Lu Wang, and Weizhu Chen. Lora: Low-rank adaptation of large language models. *arXiv preprint arXiv:2106.09685*, 2021. **1**
- [23] Eric Jang, Shixiang Gu, and Ben Poole. Categorical reparameterization with gumbel-softmax. *arXiv preprint arXiv:1611.01144*, 2016. **1**
- [24] Wouter Kool, Herke Van Hoof, and Max Welling. Stochastic beams and where to find them: The gumbel-top-k trick for sampling sequences without replacement. In *International Conference on Machine Learning*, pages 3499–3508. PMLR, 2019. **2**
- [25] Mike Lewis, Shruti Bhosale, Tim Dettmers, Naman Goyal, and Luke Zettlemoyer. BASE layers: Simplifying training of large, sparse models. In *International Conference on Machine Learning*, pages 6265–6274. PMLR, 2021. **1**
- [26] Changlin Li, Guangrun Wang, Bing Wang, Xiaodan Liang, Zhihui Li, and Xiaojun Chang. Dynamic slimmable network. In *Proceedings of the IEEE/CVF Conference on computer vision and pattern recognition*, pages 8607–8617, 2021. **1**
- [27] Vladislav Lialin, Namrata Shivagunde, Sherin Muckatira, and Anna Rumshisky. Stack more layers differently: High-rank training through low-rank updates. *arXiv preprint arXiv:2307.05695*, 2023. **1**
- [28] Chris J Maddison, Andriy Mnih, and Yee Whye Teh. The concrete distribution: A continuous relaxation of discrete random variables. *arXiv preprint arXiv:1611.00712*, 2016. **1**
- [29] Lingchen Meng, Hengduo Li, Bor-Chun Chen, Shiyi Lan, Zuxuan Wu, Yu-Gang Jiang, and Ser-Nam Lim. Advait: Adaptive vision transformers for efficient image recognition. In *Proceedings of the IEEE/CVF Conference on Computer Vision and Pattern Recognition*, pages 12309–12318, 2022. **1**

- [30] Mohammed Muqeeth, Haokun Liu, and Colin Raffel. Soft merging of experts with adaptive routing. *arXiv preprint arXiv:2306.03745*, 2023. 1
- [31] Vlad Niculae, Caio F Corro, Nikita Nangia, Tsvetomila Mihaylova, and André FT Martins. Discrete latent structure in neural networks. *arXiv preprint arXiv:2301.07473*, 2023. 1
- [32] Mathias Niepert, Pasquale Minervini, and Luca Franceschi. Implicit MLE: backpropagating through discrete exponential family distributions. *Advances in Neural Information Processing Systems*, 34:14567–14579, 2021. 2
- [33] Jonas Pfeiffer, Sebastian Ruder, Ivan Vulić, and Edoardo Maria Ponti. Modular deep learning. *arXiv preprint arXiv:2302.11529*, 2023. 1
- [34] Joan Puigcerver, Carlos Riquelme, Basil Mustafa, and Neil Houlsby. From sparse to soft mixtures of experts. *arXiv preprint arXiv:2308.00951*, 2023. 1
- [35] Zihan Qiu, Zeyu Huang, and Jie Fu. Emergent mixture-of-experts: Can dense pre-trained transformers benefit from emergent modular structures? *arXiv preprint arXiv:2310.10908*, 2023. 1
- [36] Yongming Rao, Wenliang Zhao, Benlin Liu, Jiwen Lu, Jie Zhou, and Cho-Jui Hsieh. Dynamicvit: Efficient vision transformers with dynamic token sparsification. *Advances in neural information processing systems*, 34:13937–13949, 2021. 1
- [37] Cedric Renggli, André Susano Pinto, Neil Houlsby, Basil Mustafa, Joan Puigcerver, and Carlos Riquelme. Learning to merge tokens in vision transformers. *arXiv preprint arXiv:2202.12015*, 2022. 1
- [38] Carlos Riquelme, Joan Puigcerver, Basil Mustafa, Maxim Neumann, Rodolphe Jenatton, André Susano Pinto, Daniel Keysers, and Neil Houlsby. Scaling vision with sparse mixture of experts. *Advances in Neural Information Processing Systems*, 34:8583–8595, 2021. 1
- [39] Simone Scardapane, Danilo Comminiello, Michele Scarpiniti, Enzo Baccarelli, and Aurelio Uncini. Differentiable branching in deep networks for fast inference. In *ICASSP 2020-2020 IEEE International Conference on Acoustics, Speech and Signal Processing (ICASSP)*, pages 4167–4171. IEEE, 2020. 1
- [40] Tal Schuster, Adam Fisch, Jai Gupta, Mostafa Dehghani, Dara Bahri, Vinh Tran, Yi Tay, and Donald Metzler. Confident adaptive language modeling. *Advances in Neural Information Processing Systems*, 35:17456–17472, 2022. 1
- [41] Noam Shazeer, Azalia Mirhoseini, Krzysztof Maziarz, Andy Davis, Quoc Le, Geoffrey Hinton, and Jeff Dean. Outrageously large neural networks: The sparsely-gated mixture-of-experts layer. *arXiv preprint arXiv:1701.06538*, 2017. 1
- [42] Christian Szegedy, Vincent Vanhoucke, Sergey Ioffe, Jon Shlens, and Zbigniew Wojna. Rethinking the inception architecture for computer vision. In *Proceedings of the IEEE conference on computer vision and pattern recognition*, pages 2818–2826, 2016. 2
- [43] Shawn Tan, Yikang Shen, Zhenfang Chen, Aaron Courville, and Chuang Gan. Sparse universal transformer. *arXiv preprint arXiv:2310.07096*, 2023. 1
- [44] Shengkun Tang, Yaqing Wang, Zhenglun Kong, Tianchi Zhang, Yao Li, Caiwen Ding, Yanzhi Wang, Yi Liang, and Dongkuan Xu. You need multiple exiting: Dynamic early exiting for accelerating unified vision language model. In *Proceedings of the IEEE/CVF Conference on Computer Vision and Pattern Recognition*, pages 10781–10791, 2023. 1
- [45] Surat Teerapittayanon, Bradley McDanel, and Hsiang-Tsung Kung. Branchynet: Fast inference via early exiting from deep neural networks. In *2016 23rd international conference on pattern recognition (ICPR)*, pages 2464–2469. IEEE, 2016. 1
- [46] Hugo Touvron, Matthieu Cord, and Hervé Jégou. Deit iii: Revenge of the vit. In *European Conference on Computer Vision*, pages 516–533. Springer, 2022. 2
- [47] Thomas Verelst and Tinne Tuytelaars. Dynamic convolutions: Exploiting spatial sparsity for faster inference. In *Proceedings of the IEEE/CVF conference on computer vision and pattern recognition*, pages 2320–2329, 2020. 1
- [48] Thomas Verelst and Tinne Tuytelaars. Segblocks: Block-based dynamic resolution networks for real-time segmentation. *IEEE Transactions on Pattern Analysis and Machine Intelligence*, 45(2):2400–2411, 2022. 1
- [49] Yulin Wang, Rui Huang, Shiji Song, Zeyi Huang, and Gao Huang. Not all images are worth 16x16 words: Dynamic transformers for efficient image recognition. *Advances in Neural Information Processing Systems*, 34:11960–11973, 2021. 1
- [50] Maciej Wołczyk, Bartosz Wójcik, Klaudia Bałazy, Igor T Podolak, Jacek Tabor, Marek Śmieja, and Tomasz Trzcinski. Zero time waste: Recycling predictions in early exit neural networks. *Advances in Neural Information Processing Systems*, 34:2516–2528, 2021. 1
- [51] Hao Wu, Patrick Judd, Xiaojie Zhang, Mikhail Isaev, and Paulius Micikevicius. Integer quantization for deep learning inference: Principles and empirical evaluation. *arXiv preprint arXiv:2004.09602*, 2020. 1
- [52] Wenhan Xia, Hongxu Yin, Xiaoliang Dai, and Niraj K Jha. Fully dynamic inference with deep neural networks. *IEEE Transactions on Emerging Topics in Computing*, 10(2):962–972, 2021. 1
- [53] Hongxu Yin, Arash Vahdat, Jose M Alvarez, Arun Mallya, Jan Kautz, and Pavlo Molchanov. A-vit: Adaptive tokens for efficient vision transformer. In *Proceedings of the IEEE/CVF Conference on Computer Vision and Pattern Recognition*, pages 10809–10818, 2022. 1
- [54] Seniha Esen Yuksel, Joseph N Wilson, and Paul D Gader. Twenty years of mixture of experts. *IEEE transactions on neural networks and learning systems*, 23(8):1177–1193, 2012. 1
- [55] Sangdoon Yun, Dongyoon Han, Seong Joon Oh, Sanghyuk Chun, Junsuk Choe, and Youngjoon Yoo. Cutmix: Regularization strategy to train strong classifiers with localizable features. In *Proceedings of the IEEE/CVF international conference on computer vision*, pages 6023–6032, 2019. 2
- [56] Ted Zadouri, Ahmet Üstün, Arash Ahmadian, Beyza Ermiş, Acyr Locatelli, and Sara Hooker. Pushing mixture of experts to the limit: Extremely parameter efficient moe for instruction tuning. *arXiv preprint arXiv:2309.05444*, 2023. 1

- [57] Hongyi Zhang, Moustapha Cisse, Yann N Dauphin, and David Lopez-Paz. mixup: Beyond empirical risk minimization. *arXiv preprint arXiv:1710.09412*, 2017. [2](#)
- [58] Xiaofeng Zhang, Yikang Shen, Zeyu Huang, Jie Zhou, Wenge Rong, and Zhang Xiong. Mixture of attention heads: Selecting attention heads per token. *arXiv preprint arXiv:2210.05144*, 2022. [1](#)
- [59] Zhengyan Zhang, Yankai Lin, Zhiyuan Liu, Peng Li, Maosong Sun, and Jie Zhou. Moefication: Transformer feed-forward layers are mixtures of experts. *arXiv preprint arXiv:2110.01786*, 2021. [1](#)
- [60] Yanqi Zhou, Tao Lei, Hanxiao Liu, Nan Du, Yanping Huang, Vincent Zhao, Andrew M Dai, Quoc V Le, James Laudon, et al. Mixture-of-experts with expert choice routing. *Advances in Neural Information Processing Systems*, 35:7103–7114, 2022. [1](#)
- [61] Mingjian Zhu, Kai Han, Enhua Wu, Qiulin Zhang, Ying Nie, Zhenzhong Lan, and Yunhe Wang. Dynamic resolution network. *Advances in Neural Information Processing Systems*, 34:27319–27330, 2021. [1](#)